Tena and García-Granda *SpringerPlus* (2015) 4:163
DOI 10.1186/s40064-015-0908-8

SpringerPlus
a SpringerOpen Journal

RESEARCH Open Access

Structural characterization and colour of $Mg_xCu_{3-x}V_2O_8$ ($0 \leq x \leq 3$) and $Mg_yCu_{2-y}V_2O_7$ ($0 \leq y \leq 2$) compositions

M A Tena[1*] and Santiago García-Granda[2]

Abstract

In this study, $Mg_xCu_{3-x}V_2O_8$ ($0 \leq x \leq 3$) and $Mg_yCu_{2-y}V_2O_7$ ($0 \leq y \leq 2$) compositions were synthesized by the chemical coprecipitation method and characterized by X-ray diffraction, UV–vis-NIR spectroscopy and CIE L* a* b* parameters measurements. Melting points of compounds $Cu_3V_2O_8$ and $Cu_2V_2O_7$ are 780°C and 790°C, respectively. The addition of small amounts of Mg (II), $Mg_xCu_{3-x}V_2O_8$ ($x < 1.0$) and $Mg_yCu_{2-y}V_2O_7$ ($y < 0.5$) fused compositions, was not sufficient to stabilize structures at 800°C. For the $Mg_2CuV_2O_8$ ($x = 2.0$) composition fired at 800°C, Mg (II) incorporated into the monoclinic $Cu_3V_2O_8$ structure stabilizes this crystalline phase. At 1000°C, orthorhombic $Mg_3V_2O_8$ structure from this composition was obtained. Solid solutions with orthorhombic symmetry were detected from the prepared compositions fired at 1000°C when $1.0 \leq x \leq 3.0$. The difference of coloration of Cu, Mg vanadates might be explained by the presence of a strong charge transfer band in visible spectra.

Keywords: Orthovanadate; Divanadate; Solid solutions; Structure; Colour

Background

The preparation of materials with applications on ceramic pigments industry by the conventional ceramic method presents some drawbacks. Thus, the necessary high temperatures and long soaking times give rise to loss of volatile reagents and consequently to deviation of the stoichiometric conditions of the initial systems. Some improvements were obtained with alternative synthesis methods (García et al. 2001, Tena et al. 2003). For example, no desirable brown materials were obtained from oxide mixtures in $V_xTi_{1-x}O_2$ ($x < 0.10$) rutile solid solutions with potential usefulness as gray ceramic pigments but only bluish gray colorations were obtained from gels (Tena et al. 2003). However, the ceramic pigments industry tends towards cheap and simple processing. The synthesis from mixtures of solid starting materials with addition of halides as flux agents is habitual (Sorlí et al. 2004). Alternative synthetic methods are used exceptionally. The choice of precursors materials is a possibility to obtain desired final industrial product. The bright colours of vanadates could be considered from ceramic industry to development ceramic pigments but their melting points are low. These melting points can be modified by the formation of solid solutions (West 1984). Solid solutions are very common in crystalline materials. A solid solution is basically a crystalline phase that can have variable composition.

$Cu_3V_2O_8$ and $Mg_3V_2O_8$ compounds melt incongruently at 780°C and 1212°C respectively (Fleury 1966, Clark and Morley 1976). $Mg_2V_2O_7$ melts incongruently at 1132°C (Clark and Morley 1976) and $Cu_2V_2O_7$ melts at 790°C (Fleury 1966). Considering these melting points, Mg (II) orthovanadate and Mg (II) divanadate structures can be more suitable for ceramic industry than Cu (II) orthovanadate and Cu (II) divanadate structures.

Colour is often, but not always, associated with transition metal ions. In molecular chemistry, colour can arise from two possible common causes. The d-d electronic transitions within transition metal ions give rise to many of the familiar colours of transition metal compounds,

* Correspondence: tena@uji.es
[1]Inorganic Chemistry Area, Inorganic and Organic Chemistry Department, Jaume I University, P.O. Box 224, Castellón, Spain
Full list of author information is available at the end of the article

e. g. the various shades of blue and green associated with different copper (II) complexes. Charge transfer effects in which an electron is transferred between an anion and a cation are often responsible for intense colours as in, for example, permanganate (purple) and chromates (yellow). In solids, there is an additional source of colour; it involves the transition of electrons between energy bands. Colour may be measured in a quantitative way by spectroscopic techniques. At higher frequencies than the infrared, electronic transitions associated with d-level splitting, impurity ions, crystal defects, etc., are possible. Many of these occur in the visible region and are responsible for colour.

Most of divalent metal orthovanadates of small ionic radius have orthorhombic symmetry. Copper orthovanadate presents triclinic symmetry at atmospheric pressure (Coing-Boyat 1982). A monoclinic form of this compound prepared under pressure at high temperature (4 GPa, 1173K) was described (Shannon and Calvo 1972). The structure of $Cu_3V_2O_8$ compound with monoclinic symmetry and space group $P12_1/c1$ is similar to the orthorhombic structure of $Mg_3V_2O_8$ compound with space group Cmca (Krishnamachari and Calvo 1971). Most of divalent metal divanadates, $M_2V_2O_7$, are polymorphic. Copper divanadate, $Cu_2V_2O_7$, presents orthorhombic (Calvo and Faggiani 1975), monoclinic (Mercurio-Lavaud and Bernard Frit 1973) and triclinic crystalline forms and $Mg_2V_2O_7$ presents monoclinic and triclinic symmetries (Gopal and Calvo 1974). Information about these crystal structures is included in an Additional file 1.

In this study, structural characterization of $Mg_xCu_{3-x}V_2O_8$ $(0 \le x \le 3)$ and $Mg_yCu_{2-y}V_2O_7$ $(0 \le y \le 2)$ compositions was made to investigate the possible formation of solid solutions with orthovanadate or divanadate structure. Coloration of these materials was also measured and related with structure in prepared compositions. A partial substitution of Cu (II) by Mg (II) ions might increase the melting point of materials with orthovanadates and divanadates structures. These potential solid solutions could be applied in ceramic industry.

Methods

$Mg_xCu_{3-x}V_2O_8$ $(0 \le x \le 3)$ and $Mg_yCu_{2-y}V_2O_7$ $(0 \le y \le 2)$ compositions were synthesized by the chemical coprecipitation method. The starting materials were $Cu(NO_3)_2 \cdot 2.5H_2O$ (Sigma-Aldrich, 98%), $MgCl_2.6H_2O$ (Panreac) of reagent grade chemical quality, and NH_4VO_3 (Sigma-Aldrich, 99%). The stoichiometric amount of NH_4VO_3, $Cu(NO_3)_2 \cdot 2.5H_2O$ and $MgCl_2 \cdot 6H_2O$ was added on 200 mL of water with vigorous stirring at room temperature. These starting materials were added in solid state and the concentration of the various cations is different in each prepared composition. After that, a solution of ammonium hydroxide was added dropwise until pH = 8. The obtained precipitates were dried by an infrared lamp and dry samples were fired at 300°C for 12 hours, 600°C for 12 hours, 800°C for 1 hour and 1000°C for 1 hour.

The resulting materials were examined by X-ray diffraction with CuKα radiation to study the development

Table 1 Structural information of Cu and Mg orthovanadates and divanadates

Structure	ICSD* reference	Crystalline system	Standard unit cell* (Å and degrees)	Standard space group	Z
$Cu_3V_2O_8$	27184	Triclinic	a = 5.196 (4), b = 5.355 (1), c = 6.505 (4), α = 69.22 (3), β = 88.69 (4), γ = 68.08 (3)	P −1	1
$Cu_3V_2O_8$	27310	Monoclinic	a = 6.2493 (9), b = 7.9936 (9), c = 6.378 (1), β = 111.49 (1)	P 1 2_1/c 1	2
$MgCu_2V_2O_8$	404852	Monoclinic	a = 6.453 (1), b = 8.342 (2), c = 11.517 (2), β = 90.44 (2)	P 1 2_1/c 1	4
$Mg_2CuV_2O_8$	404851	Monoclinic	a = 6.167 (3), b = 8.172 (5), c = 6.400 (3), β = 116.22 (3)	P 1 2_1/c 1	2
$Mg_3V_2O_8$	156155	Orthorhombic	a = 6.0814 (7), b = 11.469 (1), c = 8.337 (1)	C m c a	4
α-$Cu_2V_2O_7$	34756	Orthorhombic	a = 8.411 (5), b = 20.68 (1), c = 6.448 (5)	F d d 2	8
β-$Cu_2V_2O_7$	158375	Monoclinic	a = 7.6890 (8), b = 8.0289 (9), c = 10.1065 (8), β = 110.252 (7)	C 1 2/c 1	4
γ-$Cu_2V_2O_7$	171028	Triclinic	a = 5.087 (1), b = 5.823 (1), c = 9.402 (2), α = 99.780 (3), β = 97.253 (3), γ = 97.202 (3)	P −1	2
$Cu_{1.5}Mg_{0.5}V_2O_7$	69731	Monoclinic	a = 7.660 (6), b = 8.089 (8), c = 10.117 (9), β = 110.6 (1)	C 1 2/c 1	4
$Cu_{1.33}Mg_{0.67}V_2O_7$	69732	Monoclinic	a = 7.645 (4), b = 8.095 (3), c = 10.119 (3), β = 110.54 (3)	C 1 2/c 1	4
α-$Mg_2V_2O_7$	93603	Monoclinic	a = 6.599 (1), b = 8.406 (1), c = 9.472 (2), β = 100.6085 (4)	P 1 2_1/c 1	4
$Mg_2V_2O_7$	2321	Triclinic	a = 4.912 (2), b = 5.414 (3), c = 10.669 (7), α = 100.36 (4), β = 102.82 (4), γ = 98.58 (4)	P −1	2

* Inorganic Crystal Structure Database (ICSD) (2013).

of the crystalline phases at different temperatures. A structure profile refinement was carried out by the Rietveld method (Fullprof.2 k computer program) (Rietveld 1969, Rodriguez-Carvajal 2012, Chapon and Rodriguez-Carvajal 2008). Unit cell parameters and interatomic distances (M-O and V-O) in divanadates and orthovanadates structures were obtained from $Mg_xCu_{3-x}V_2O_8$ ($0 \le x \le 3$) and $Mg_yCu_{2-y}V_2O_7$ ($0 \le y \le 2$) fired compositions to investigate the possibility of formation of solid solution in these synthetic conditions. The diffraction patterns were collected running from 5 to 110 $^o2\theta$, using monochromatic CuK_α radiation, a step size of 0.02 $^o2\theta$ and a sampling time of 10 s. The initial structural information was obtained of the Inorganic Crystal Structure Database (Inorganic Crystal Structure Database ICSD 2013). Table 1 includes the reference ICSD to every structure. This initial structural information also appears in the references (Coing-Boyat 1982, Shannon and Calvo 1972, Krishnamachari and Calvo 1971, Calvo and Faggiani 1975, Mercurio-Lavaud and Bernard Frit 1973, Gopal and Calvo 1974) for the main structures of this study. Dicvol program (Boultif and Loüer 2007) was used to obtain initial cell parameters in some compositions.

UV–vis-NIR spectroscopy (diffuse reflectance) allows the Cu (II) site and the V (V)-O and Cu (II)-O charge bands in samples to be studied. A Jasco V-670 spectrophotometer

Table 2 Evolution of crystalline phases with temperature in $Mg_xCu_{3-x}V_2O_8$ ($0 \le x \le 3$) samples

x	T (°C)	Crystalline phases
0.00	300	C2(s), C1(vw)
0.50	300	C2(s), MT(w), C1(vw)
1.00	300	CM(m), M(w), C2(vw)
1.50	300	CM(m)
2.00	300	M(m), CM(w)
2.50	300	M(m), MT(w)
3.00	300	M(m), MT(w)
0.00	600	CT(s), C1(m), C2(m)
0.50	600	CT(m), C2(w), M(vw), C1(vw)
1.00	600	CT(m), M(m), C2(w), MO(w), CM(vw)
1.50	600	CM(m)
2.00	600	CM(m), MO(w)
2.50	600	MO(m), M(vw)
3.00	600	MO(m), M(w)
1.00	800	MC(s)
1.50	800	CM(s), MC(s), C2(vw)
2.00	800	CM(s)
2.50	800	MO(s), M(vw)
3.00	800	MO(s), MT(w)
1.00	1000	MO(m), CM(w), M(vw)
1.50	1000	MO(m), CM(w), M(w)
2.00	1000	MO(m), M(w), MC(vw), CT(vw)
2.50	1000	MO(s), MT(vw)
3.00	1000	MO(s), MT(w)

Crystalline phases: CT = $Cu_3V_2O_8$ (triclinic), CM = $Cu_3V_2O_8$ (monoclinic), MC = $MgCu_2V_2O_8$ (monoclinic), MO = $Mg_3V_2O_8$ (orthorhombic), C1 = α-$Cu_2V_2O_7$ (orthorhombic), C2 = β-$Cu_2V_2O_7$ (monoclinic), C3 = γ-$Cu_2V_2O_7$ (triclinic), M = α-$Mg_2V_2O_7$ (monoclinic), MT = $Mg_2V_2O_7$ (triclinic).
Diffraction peak intensity: s = strong, m = medium, w = weak, vw = very weak.

Table 3 Evolution of crystalline phases with temperature in $Mg_yCu_{2-y}V_2O_7$ ($0 \le y \le 2$) samples

y	T (°C)	Crystalline phases
0.00	300	C2(m), CT(m), M2(m), C1(w), CM(w), C3(vw)
0.25	300	C2(m), C3(m), M3(m)
0.50	300	C3(m), M2(m), M1(m), C2(w), M3(w), C1(vw)
0.75	300	CM(s), M2(m), C2(w), C3(w)
1.00	300	C3(w), M1(w), CM(vw)
1.25	300	CM(s), N(s), C2(vw)
1.50	300	C3(m), CM(vw), M3(w)
1.75	300	N(s), CM(m), C2(vw)
2.00	300	N(s), MT(w)
0.00	600	C1(s)
0.25	600	C2(s), C1(w)
0.50	600	C2(s), C2′(m), M3(w)
0.75	600	M3(s), C2(m), C2′(m)
1.00	600	M3(m), C2(m)
1.25	600	C2(m), M4(m), M3(w)
1.50	600	C2(m), M4(m), M1(w)
1.75	600	M1(s), C2(w), M4(w)
2.00	600	M1(s), M2(w)
0.50	800	C2(s), M4(m), M2(w)
0.75	800	C2(s), M3(m), C3(w)
1.00	800	M4(s), C2(w)
1.25	800	M4(s), C2(w), M3(w)
1.50	800	C1(s), M4(m), MT(vw)
1.75	800	MT(m), M4(m)
2.00	800	MT(m), M4(m)
1.50	1000	M1(m), MT(m), C2(w)
1.75	1000	M1(s), MT(w), C2(vw)
2.00	1000	MT(m), M1(w), MO(w)

Crystalline phases: C1 = α-$Cu_2V_2O_7$ (orthorhombic), C2 = β-$Cu_2V_2O_7$ (monoclinic, C2: β < 110.6°, C2′: β > 110.6°), C3 = γ-$Cu_2V_2O_7$ (triclinic), CT = $Cu_3V_2O_8$ (triclinic), CM = $Cu_3V_2O_8$ (monoclinic), M = α-$Mg_2V_2O_7$ (monoclinic, M1: β =100.6-102.0°, M2: β = 98.0-99.6°, M3: β = 94.5-97.0°, M4: β = 88.0-92.0°), MT = $Mg_2V_2O_7$ (triclinic), N = α-$Mn_2V_2O_7$ (triclinic, P $\bar{1}$, Z =4 with all atoms in 2i sites, ICSD-81993), MO = $Mg_3V_2O_8$ (orthorhombic).
Diffraction peak intensity: s = strong, m = medium, w = weak, vw = very weak.

was used to obtain the UV–vis-NIR (ultraviolet visible near infrared) spectra in the 200 to 2500 nm range. X-Rite spectrophotometer (SP60, an illuminant D65, an observer 10°, and a reference sample of MgO) was used to obtain CIEL*a*b* colour parameters on fired samples: L* is the lightness axis (black (0) → white (100)), a* the green (−) → red (+) axis, and b* is the blue (−) → yellow (+) axis (CIE 1971).

Results and discussion

Tables 2 and 3 show crystalline phase evolution with composition and temperature in $Mg_xCu_{3-x}V_2O_8$ ($0 \le x \le 3$) and $Mg_yCu_{2-y}V_2O_7$ ($0 \le y \le 2$) compositions. XRD patterns from $Mg_xCu_{3-x}V_2O_8$ and $MgyCu_{2-y}V_2O_7$ compositions are shown in Additional files 2 and 3.

In $Mg_xCu_{3-x}V_2O_8$ ($0 \le x < 1.0$) compositions the major crystalline phase is the triclinic $Cu_3V_2O_8$ polymorph

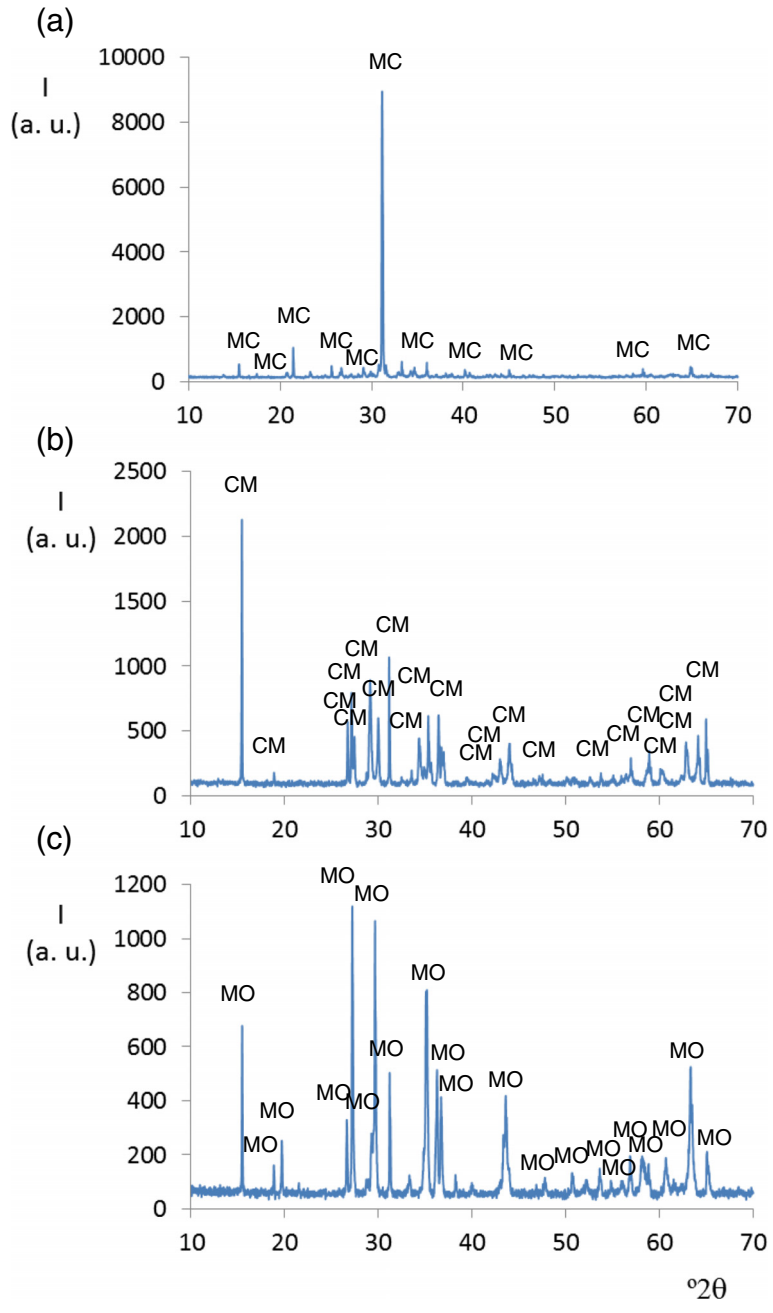

Figure 1 Diffractograms from $Mg_xCu_{3-x}V_2O_8$ compositions at 800°C. Diffraction maxima from the major crystalline phase in : **(a)** x = 1.0, $MgCu_2V_2O_8$; **(b)** x = 2.0, $Mg_2CuV_2O_8$ and **(c)** x = 2.5, $Mg_{2.5}Cu_{0.5}V_2O_8$ compositions. Crystalline phases: MC ($MgCu_2V_2O_8$, monoclinic), CM ($Cu_3V_2O_8$, monoclinic) and MO ($Mg_3V_2O_8$, orthorhombic).

at 600°C. $Cu_3V_2O_8$ compound melts incongruently at 780°C. This fact can explain the melting of samples with a presence higher than 50% in $Cu_3V_2O_8$ triclinic crystalline phase (small amount of Mg in compositions). This crystalline phase with triclinic structure is not detected in samples fired at 800 and 1000°C.

A crystalline phase with $Cu_3V_2O_8$ structure and monoclinic symmetry was obtained at 300 and 600°C in compositions with $1.0 \leq x \leq 2.0$. This crystalline phase with monoclinic $Cu_3V_2O_8$ structure is also present when $1.5 \leq x \leq 2.0$ at 800°C. The crystalline phase with the structure of $MgCu_2V_2O_8$ compound ($\beta = 90.44$ (2) and $Z = 4$) is detected when $1.0 \leq x \leq 2.0$ at 800°C but the crystalline phase with the ordered metal distributions in $Mg_2CuV_2O_8$ compound ($\beta = 116.22$ (3), $Z = 2$, Cu1 in 2a sites and Mg1 in 4e sites, ICSD-404851) is not detected

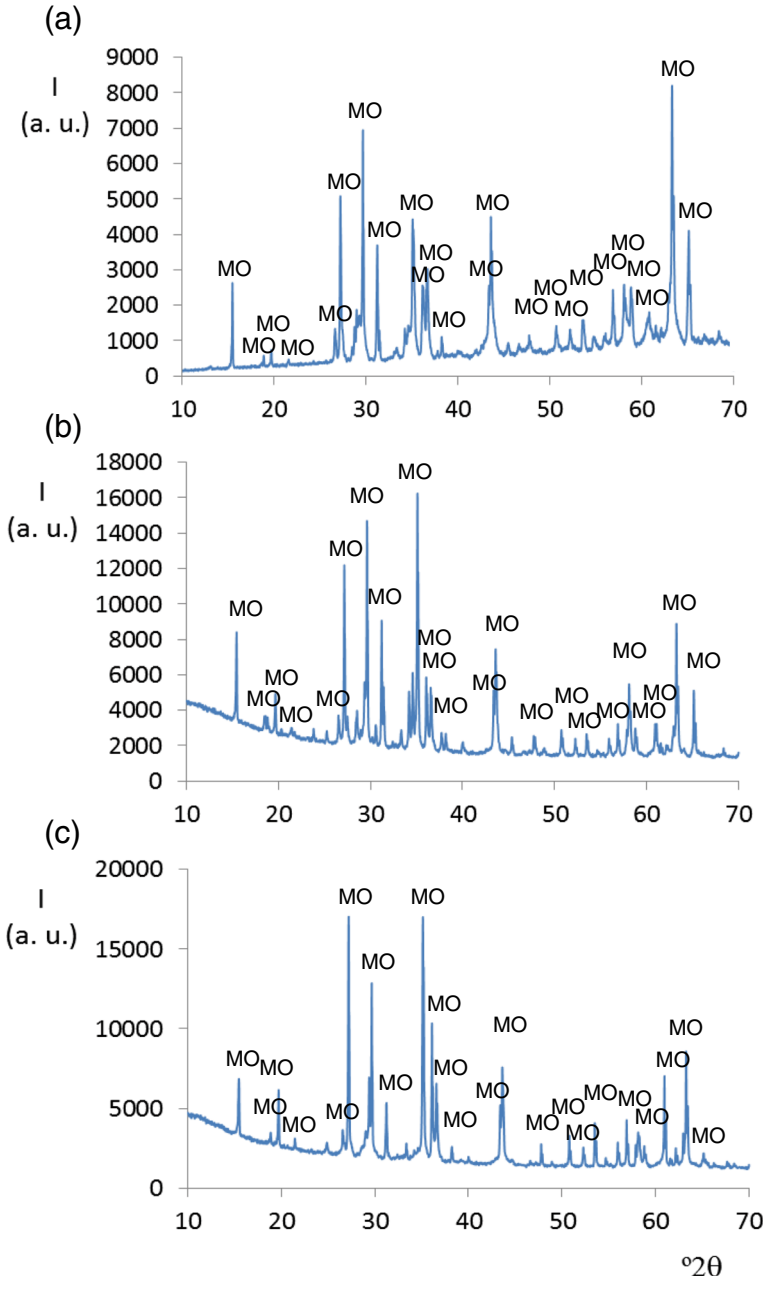

Figure 2 Diffractograms from $Mg_xCu_{3-x}V_2O_8$ compositions at 1000°C. Diffraction maxima from the major phase in: **(a)** x = 1.0, $MgCu_2V_2O_8$; **(b)** x = 2.0, $Mg_2Cu_2V_2O_8$ and **(c)** x = 2.5, $Mg_{2.5}Cu_{0.5}V_2O_8$ compositions. MO: orthorhombic $Mg_3V_2O_8$ crystalline phase.

in conditions of this study. In the prepared $Mg_2CuV_2O_8$ composition ($Mg_xCu_{3-x}V_2O_8$ with x =2.0), crystalline phase with $Cu_3V_2O_8$ structure and monoclinic symmetry (Z = 2 and M1 (M1 = Mg, Cu) in 2b sites and M2 (M2 = Mg, Cu) in 4e sites) is the only crystalline phase detected at 800°C. Figure 1 shows the major crystalline phase detected in $MgCu_2V_2O_8$ (x = 1.0), $Mg_2CuV_2O_8$ (x = 2.0) and $Mg_{2.5}Cu_{0.5}V_2O_8$ (x = 2.5) compositions fired at 800°C.

Crystalline phase with orthorhombic $Mg_3V_2O_8$ structure is obtained when $2.0 \le x \le 3.0$ at 600°C and when $2.5 \le x \le 3.0$ at 800°C. At 1000°C, this phase is the major crystalline phase in the unfused samples ($x \ge 1.0$). Figure 2 shows the positions of diffraction lines and their intensities from $Mg_xCu_{3-x}V_2O_8$ compositions with x = 1.0, x = 2.0 and x = 2.5 fired at 1000°C. The orthorhombic $Mg_3V_2O_8$ crystalline phase is the major phase in them.

Cu divanadates and Mg divanadates are present together with Cu and Mg orthovanadates in some samples.

Crystalline phase with α-$Cu_2V_2O_7$ structure (orthorhombic symmetry) is only present in $Mg_yCu_{2-y}V_2O_7$ compositions when $y < 0.5$ at 600°C. These compositions melt at 800°C. Diffraction peak intensity associated with this crystalline phase is weak or very weak at 300°C.

Presence of crystalline phase with β-$Cu_2V_2O_7$ structure (monoclinic symmetry) is more extended than the crystalline phase with α-$Cu_2V_2O_7$ structure in the prepared compositions. At 300°C, crystalline phase with β-$Cu_2V_2O_7$ structure is present when $y < 0.5$ with diffraction peaks of medium intensity. This crystalline phase is present when $0.25 \le y < 1.50$ at 600°C and when $0.50 \le y \le 0.75$ with diffraction peak of strong or medium intensity. Figure 3 shows graphical result of the diffraction profile refinement by Rietveld's method from the $Mg_{0.25}Cu_{1.75}V_2O_7$ composition fired at 600°C.

Crystalline phase with γ-$Cu_2V_2O_7$ structure (triclinic symmetry) is present in compositions when $0.25 \le y \le 0.50$ at 300°C but its intensity of diffraction peak is weak at 600 and 800°C (Table 3).

In $Mg_yCu_{2-y}V_2O_7$ compositions fired at 300°C, the assignation to α- $Mn_2V_2O_7$ structure of a crystalline phase detected when $y \ge 1.25$ might be explained by the existence of a polymorph of $Mg_2V_2O_7$ compound with this structure. It was not detected any match with the existing single-crystal related in the bibliography. Synthesis of single-crystal is the most used method in synthesis of vanadates.

Crystalline phase with α-$Mg_2V_2O_7$ structure (monoclinic symmetry) is detected in a compositional range more extended than the crystalline phase with triclinic $Mg_2V_2O_7$ structure from $Mg_yCu_{2-y}V_2O_7$ prepared compositions. Crystalline phase with monoclinic α-$Mg_2V_2O_7$ structure is identified when $0.75 \le y \le 2.00$ at 600°C, when $0.50 \le y \le 2.00$ at 800°C, and when $1.50 \le y \le 2.00$ at 1000°C.

Crystalline phase with triclinic $Mg_2V_2O_7$ structure is observed when $1.5 \le y \le 2.00$ in compositions fired at 800°C and only when y = 2.0 at 300°C.

Tables 4, 5, 6, 7, 8 and 9 show the unit cell parameters and weight fractions in crystalline phases with weight fractions higher than 8% from samples fired at 600, 800 and 1000°C. The variation of these parameters with composition confirms the formation of solid solutions.

From $Mg_xCu_{3-x}V_2O_8$ compositions solid solutions with triclinic $Cu_3V_2O_8$ structure are obtained when $0.0 \le x \le 1.0$ at 600°C. At this temperature, the c unit cell parameter increases slightly with the replacement of Cu (II) ion by a slightly smaller one (Mg (II)) from $Mg_xCu_{3-x}V_2O_8$ compositions when $0.0 \le x \le 1.0$. Ionic radii values do not explain this fact. A slight contraction of unit cell is expected. Structural distortion might explain the c increase with incorporation of Mg (II) ions in a structure (Tena 2012).

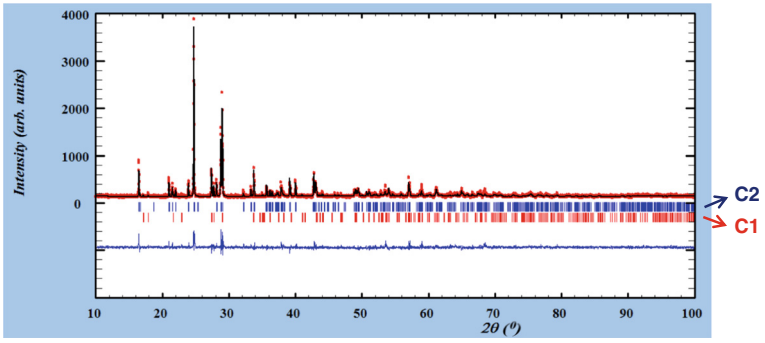

Figure 3 An example of the diffraction profile refinement. The diffraction profile refinement by Rietveld's method from $Mg_{0.25}Cu_{1.75}V_2O_7$ composition fired at 600°C. Crystalline phases: α-$Cu_2V_2O_7$ (C1) and β- $Cu_2V_2O_7$ (C2).

Table 4 Unit cell parameters in crystalline phases with weight fractions higher than 8% from $Mg_xCu_{3-x}V_2O_8$ ($0 \leq x \leq 3$) compositions fired at 600°C/12 h

x	Crystalline phases (weight fractions)	Unit cell parameters (Å and degrees)
0.00	CT (75.02 %)	a = 5.18451(7) b = 5.34518(8) c = 6.51005(7)
		α = 69.261(1) β = 88.644(1) γ= 68.99(1)
	C1 (12.83 %)	a = 8.4016(3) b = 20.666(1) c = 6.4433(2)
		α = 90.00 β = 90.00 γ = 90.0
	C2 (12.16 %)	a = 7.6982(6) b = 8.0361(9) c = 10.112(1)
		α = 90.00 β = 110.29(1) γ = 90.00
0.50	CT (64.09 %)	a = 5.1861(2) b = 5.3448(2) c = 6.5457(2)
		α = 69.039(3) β = 88.500(4) γ = 68.036(3)
	C2 (21.23 %)	a = 7.6404(7) b = 8.1244(9) c = 10.116(1)
		α = 90.00 β = 110.66(1) γ = 90.00
	M (11.41 %)	a = 6.611(1) b = 8.314(2) c = 9.483(1)
		α = 90.00 β = 100.54(2) γ = 90.00
1.00	CT (23.62 %)	a = 5.1925(3) b = 5.3492(3) c = 6.5674(3)
		α = 68.997(5) β = 88.449(6) γ = 67.980(5)
	C2 (19.24 %)	a = 7.6147(5) b = 8.1294(6) c = 10.1159(6)
		α = 90.00 β = 110.374(6) γ = 90.00
	MO (18.80 %)	a = 6.0533(5) b = 11.098(1) c = 8.4009(8)
		α = 90.00 β = 90.00 γ = 90.00
	M (26.46 %)	a = 6.5954(4) b = 8.3555(4) c = 9.4997(6)
		α = 90.00 β = 100.520(5) γ = 90.00
	CM (13.71 %)	a = 6.1842(7) b = 8.084(1) c = 6.3181(9)
		α = 90.00 β = 111.38(1) γ = 90.00
1.50	CM (100 %)	a = 6.3729(1) b = 8.1626(2) c = 6.1790(1)
		α = 90.00 β = 115,608(2) γ = 90.00
2.00	CM (73.01 %)	a = 6.5984(3) b = 8.1901(3) c = 6.1459(3)
		α = 90.00 β = 119.656(2) γ = 90.00
	MO (26.99 %)	a = 6.0787(3) b = 11.4674(8) c = 8.2078(5)
		α = 90.00 β = 90.00 γ = 90.00
2.50	MO (92.55 %)	a = 6.0975(1) b = 11.4523(2) c = 8.2555(2)
		α = 90.00 β = 90.00 γ = 90.00
3.00	MO (80.94 %)	a = 6.0613(3) b = 11.4395(5) c = 8.3115(4)
		α = 90.00 β = 90.00 γ = 90.00
	M (19.06 %)	a = 6.6051(5) b = 8.4106(6) c = 9.4815(8)
		α = 90.00 β = 100.626(8) γ = 90.00

Crystalline phases: CT = $Cu_3V_2O_8$ (triclinic), CM = $Cu_3V_2O_8$ (monoclinic), MO = $Mg_3V_2O_8$ (orthorhombic), C1 = α-$Cu_2V_2O_7$ (orthorhombic), C2 = β-$Cu_2V_2O_7$ (monoclinic), M = α-$Mg_2V_2O_7$ (monoclinic).

Variation of unit cell parameters obtained from $Mg_xCu_{3-x}V_2O_8$ ($x \geq 1.0$) compositions fired at 800°C is noticeable in monoclinic $Cu_3V_2O_8$ structure (detected when $1.5 \leq x \leq 2.0$) and it indicates the formation of solid solutions with monoclinic $Cu_3V_2O_8$ structure in $1.5 \leq x \leq 2$ compositional range at 600°C and 800°C.

Table 5 Unit cell parameters in crystalline phases with weight fractions higher than 8% from $Mg_xCu_{3-x}V_2O_8$ ($0 \leq x \leq 3$) compositions fired at 800°C/1 h

x	Crystalline phases (weight fractions)	Unit cell parameters (Å and degrees)
1.00	MC (100%)	a = 6.4444 (1) b = 8.2992 (1) c = 11.4842 (2)
		α = 90.00 β = 90.61 γ = 90.00
1.50	CM (55.49%)	a = 6.3869 (3) b = 8.1575 (4) c = 6.1600 (3)
		α = 90.00 β = 116.308 (3) γ = 90.00
	MC (40.82%)	a = 6.4472 (1) b = 8.2960 (2) c = 11.4933 (2)
		α = 90.00 β = 90.479 (2) γ = 90.00
2.00	CM (100%)	a = 6.6120 (1) b = 8.1901 (1) c = 6.1525 (1)
		α = 90.00 β = 119.795 (1) γ = 90.00
2.50	MO (92.55%)	a = 6.0963 (1) b = 11.4581 (2) c = 8.2556 (1)
		α = 90.00 β = 90.00 γ = 90.00
3.00	MO (76.55%)	a = 6.06485 (6) b = 11.4416 (1) c = 8.31576 (8)
		α = 90.00 β = 90.00 γ = 90.00
	MT (23.45%)	a = 4.9304 (2) b = 5.4199 (2) c = 10.6787 (4)
		α = 100.321 (3) β = 102.808 (3) γ = 98.640 (3)

Crystalline phases: CM = $Cu_3V_2O_8$ (monoclinic), MC = $MgCu_2V_2O_8$ (monoclinic), MO = $Mg_3V_2O_8$ (orthorhombic), C2 = β-$Cu_2V_2O_7$ (monoclinic), MT = $Mg_2V_2O_7$ (triclinic).

Table 6 Unit cell parameters in crystalline phases with weight fractions higher than 8% from $Mg_xCu_{3-x}V_2O_8$ ($0 \leq x \leq 3$) compositions fired at 1000°C/1 h

x	Crystalline phases (weight fractions)	Unit cell parameters (Å and degrees)
1.00	MO (84.55%)	a = 6.0999 (2) b = 11.4633 (4) c = 8.2642 (3)
		α = 90.00 β = 90.90 γ = 90.00
	CM (12.12%)	a = 6.4805 (9) b = 8.458 (1) c = 6.2031 (8)
		α = 90.00 β = 117.29 (1) γ = 90.00
1.50	MO (66.10%)	a = 6.0850 (2) b = 11.4556 (4) c = 8.2858 (2)
		α = 90.00 β = 90.90 γ = 90.00
	CM (17.35%)	a = 6.5138 (7) b = 8.590 (1) c = 6.2116 (8)
		α = 90.00 β = 117.495 (9) γ = 90.00
	M (16.54%)	a = 6.5786 (6) b = 8.4263 (7) c = 9.5107 (9)
		α = 90.00 β = 100.49 (1) γ = 90.00
2.00	MO (78.31%)	a = 6.0826 (1) b = 11.4538 (3) c = 8.2864 (2)
		α = 90.00 β = 90.00 γ = 90.00
	M (9.13%)	a = 6.1867 (6) b = 8.2179 (7) c = 6.3129 (5)
		α = 90.00 β = 112.016 (8) γ = 90.00
2.50	MO (96.02%)	a = 6.0775 (1) b = 11.4473 (2) c = 8.2813 (1)
		α = 90.00 β = 90.00 γ = 90.00
3.00	MO (77.73%)	a = 6.06118 (5) b = 11.4365 (1) c = 8.31278 (7)
		α = 90.00 β = 90.00 γ = 90.00
	MT (22.27%)	a = 4.9278 (2) b = 5.4169 (2) c = 10.6733 (4)
		α = 100.326 (2) β = 102.779 (3) γ = 98.632 (2)

Crystalline phases: CM = $Cu_3V_2O_8$ (monoclinic), MO = $Mg_3V_2O_8$ (orthorhombic), M = $Mg_2V_2O_7$ (monoclinic), MT = $Mg_2V_2O_7$ (triclinic).

Table 7 Unit cell parameters in crystalline phases with weight fractions higher than 8% from $Mg_yCu_{2-y}V_2O_7$ ($0 \le y \le 2$) compositions fired at 600°C/12 h

y	Crystalline phases (weight fractions)	Unit cell parameters (Å and degrees) a / b / c // α / β / γ
0.000	C1 (100%)	8.40244 (8) / 20.6701 (2) / 6.44418 (5) // 90.00 / 90.00 / 90.00
0.250	C2 (87.6%)	7.67549 (8) / 8.0734 (1) / 10.1196 (2) // 90.00 / 110.437 (1) / 90.00
	C1 (12.4%)	8.3703 (3) / 20.6942 (8) / 6.4551 (3) // 90.00 / 90.00 / 90.00
0.500	C2 (63.1%)	7.6554 (1) / 8.1002 (1) / 10.1168 (2) // 90.00 / 110.550 (1) / 90.00
	C2'(26.8%)	7.6219 (4) / 8.0881 (6) / 10.1139 (6) // 90.00 / 110.655 (5) / 90.00
	M3 (10.1%)	6.7623 (6) / 8.4212 (7) / 9.3331 (9) // 90.00 / 95.61 (1) / 90.00
0.750	M3 (50.51%)	6.7701 (5) / 8.4666 (5) / 9.3134 (7) // 90.00 / 96.577 (7) / 90.00
	C2'(29.1%)	7.6322 (4) / 8.0720 (5) / 10.1722 (7) // 90.00 / 111.164 (5) / 90.00
	C2 (20.4%)	7.6410 (4) / 8.1202 (5) / 11.1141 (5) // 90.00 / 110.629 (5) / 90.00
1.000	M3 (54.4%)	6.8418 (4) / 8.4116 (4) / 9.3644 (5) // 90.00 / 95.904 (5) / 90.00
	C2 (45.6%)	7.6091 (4) / 8.0465 (3) / 10.1275 (5) // 90.00 / 110.048 (5) / 90.00
1.250	C2 (36.4%)	7.6115 (2) / 8.0629 (2) / 10.1148 (3) // 90.00 / 109.804 (3) / 90.00
	M4 (40.0%)	6.8263 (2) / 8.0816 (3) / 9.3090 (3) // 90.00 / 88.438 (3) / 90.00
	M3 (23.6%)	6.8846 (3) / 8.4130 (4) / 9.2537 (5) // 90.00 / 95.778 (4) / 90.00
1.500	C2 (37.4%)	7.5684 (3) / 8.0539 (3) / 10.1486 (4) // 90.00 / 109.879 (4) / 90.00
	M4 (42.3%)	6.8291 (2) / 8.0591 (3) / 9.3291 (3) // 90.00 / 88.249 (3) / 90.00
	M1 (20.3%)	6.5895 (5) / 8.3913 (6) / 9.4963 (7) // 90.00 / 100.397 (7) / 90.00
1.750	M1 (73.1%)	6.58498 (9) / 8.3914 (1) / 9.4872 (1) // 90.00 / 100.462 (1) / 90.00
	M4 (15.1%)	6.8308 (4) / 8.0534 (4) / 9.3113 (5) // 90.00 / 88.705 (6) / 90.00
	C2 (11.8%)	7.5662 (5) / 8.0592 (5) / 10.1427 (6) // 90.00 / 109.864 (6) / 90.00
2.000	M1 (83.9%)	6.60534 (6) / 8.41437 (8) / 9.48264 (9) // 90.00 / 100.6104 (8) / 90.00
	M2 (16.1%)	6.6639 (2) / 8.4361 (3) / 9.5745 (3) // 90.00 / 99.446 (3) / 90.00

Crystalline phases: C1 = α-$Cu_2V_2O_7$, C2 = β-$Cu_2V_2O_7$ (monoclinic, C2: β < 110.6°, C2': β > 110.6°), M = α-$Mg_2V_2O_7$ (monoclinic, M1: β = 100.0-100.6°, M2: β = 98.0-99.6°, M3: β = 94.5-97.0°, M4: β = 88.0-92.0°).

Table 8 Unit cell parameters in crystalline phases with weight fractions higher than 8% from $Mg_yCu_{2-y}V_2O_7$ ($0 \le y \le 2$) compositions fired at 800°C/1 h

y	Crystalline phases (weight fractions)	Unit cell parameters (Å and degrees) a / b / c // α / β / γ
0.500	C2 (56.8%)	7.6430 (3) / 8.1076 (3) / 10.1147 (4) // 90.00 / 110.589 (4) / 90.00
	M4 (26.3%)	6.719 (1) / 8.553 (1) / 9.846 (2) // 90.00 / 91.33 (2) / 90.00
	M2 (16.9%)	6.936 (1) / 8.423 (1) / 9.793 (2) // 90.00 / 98.32 (1) / 90.00
0.750	M3 (48.4%)	6.9060 (4) / 8.3131 (5) / 9.5450 (5) // 90.00 / 95.346 (7) / 90.00
	C2 (36.0%)	7.6308 (4) / 8.1127 (5) / 10.0542 (7) // 90.00 / 110.389 (6) / 90.00
	C3 (15.1%)	4.9809 (5) / 5.8341 (6) / 10.933 (1) // 101.554 (8) / 96.517 (7) / 95.032 (8)
1.000	M4 (91.3%)	6.7766 (4) / 8.4899 (4) / 9.1447 (6) // 90.00 / 88.294 (5) / 90.00
	C2 (8.7%)	7.542 (2) / 8.083 (2) / 10.0574 (2) // 90.00 / 110.59 (2) / 90.00
1.250	M4 (79.9%)	6.81447 (7) / 8.11262 (8) / 9.30424 (9) // 90.00 / 88.444 (1) / 90.00
	C2 (13.9%)	7.6192 (3) / 8.0576 (4) / 10.1113 (4) // 90.00 / 109.689 (4) / 90.00
1.500	C1 (63.8%)	8.3392 (1) / 20.8256 (3) / 6.44642 (9) // 90.00 / 90.00 / 90.00
	M4 (32.1%)	6.7458 (3) / 7.8414 (3) / 9.2234 (3) // 90.00 / 90.890 (3) / 90.00
1.750	M4 (59.3%)	6.7825 (3) / 8.0761 (3) / 9.3084 (4) // 90.00 / 89.448 (4) / 90.00
	MT (40.7%)	4.9343 (4) / 5.4102 (5) / 10.7164 (9) // 99.866 (7) / 102.996 (5) / 98.743 (7)
2.000	M4 (59.3%)	6.7823 (1) / 8.0669 (2) / 9.3201 (2) // 90.00 / 89.345 (2) / 90.00
	MT (40.7%)	4.9354 (2) / 5.4094 (2) / 10.7145 (5) // 99.874 (3) / 102.959 (3) / 98.756 (3)

Crystalline phases: C1 = α-$Cu_2V_2O_7$, C2 = β-$Cu_2V_2O_7$ (monoclinic, C2: β < 110.6°, C2': β > 110.6°), C3 = γ-$Cu_2V_2O_7$ (triclinic), M = α-$Mg_2V_2O_7$ (monoclinic, M1: β = 100.0-100.6°, M2: β = 98.0-99.6°, M3: β = 94.5-97.0°, M4: β = 88.0-92.0°), MT = γ-$Mg_2V_2O_7$ (triclinic).

Solid solutions with orthorhombic $Mg_3V_2O_8$ structure are also obtained when $2.5 \le x \le 3.0$ at 600, 800°C and when $1.0 \le x \le 3.0$ at 1000°C. Figure 4 shows unit cell parameters and interatomic distances in Mg orthovanadate structure (orthorhombic symmetry) obtained from $Mg_xCu_{3-x}V_2O_8$ samples fired at 1000°C/1 h. At 1000°C, the a and b unit cell parameters decrease with the replacement of Cu (II) ion by a slightly smaller one (Mg (II)). Average changes of interatomic distances are very slight. Changes in intensities with composition (Figure 2) are due to changes in both the atomic coordinates and the Mg/Cu ratio in these sites in orthorhombic $Mg_3V_2O_8$ structure when solid solutions are formed. These solid solutions are the most stable solid

Table 9 Unit cell parameters in crystalline phases with weight fractions higher than 8% from $Mg_yCu_{2-y}V_2O_7$ ($0 \leq y \leq 2$) compositions fired at 1000°C/1 h

y	Crystalline phases weight fractions)	Unit cell parameters (Å and degrees) a / b / c // α / β / γ
1.500	MT (41.6%)	4.9331 (2) / 5.4122 (3) / 10.7005 (5) // 100.037 (4) / 102.907 (3) / 98.777 (4)
	M1 (39.7%)	6.6011 (4) / 8.4011 (4) / 9.5027 (5) // 90.00 / 100.394 (5) / 90.00
1.750	M1 (81.1%)	6.5951 (1) / 8.4057 (2) / 9.5075 (2) // 90.00 / 100.427 (2) / 90.00
	MT (16.5%)	4.9318 (4) / 5.4130 (5) / 10.7219 (9) // 100.109 (8) / 102.908 (6) / 98.769 (7)
2.000	MT (69.0%)	4.9276 (2) / 5.4164 (2) / 10.6697 (4) // 100.318 (2) / 102.785 (3) / 98.617 (3)
	MO (17.4%)	6.0832 (4) / 10.8818 (5) / 8.6212 (5) // 90.00 / 90.00 / 90.00
	M1 (13.6%)	6.4596 (7) / 8.5135 (8) / 9.403 (1) // 90.00 / 102.00 (1) / 90.00

Crystalline phases: M = α-$Mg_2V_2O_7$ (monoclinic, M1: β = 100.6-102.0°), MT = γ-$Mg_2V_2O_7$ (triclinic), MO = $Mg_3V_2O_8$ (orthorhombic).

solutions obtained in this study from $Mg_xCu_{3-x}V_2O_8$ compositions.

From unit cell parameters values obtained in $Mg_yCu_{2-y}V_2O_7$ compositions, the formation of two kinds of solid solutions with monoclinic β-$Cu_2V_2O_7$ and monoclinic α-$Mg_2V_2O_7$ structures can be confirmed. Two crystalline phases with the same structure (β-$Cu_2V_2O_7$ or α-$Mg_2V_2O_7$) are detected in some samples (Tables 7 and 8). This fact indicates that the composition of these two crystalline phase (C2: β < 110.6 ° and C2': β > 110.6° with β-$Cu_2V_2O_7$ structure or two of M1: β = 100.0-100.6°, M2: β = 98.0-99.6°, M3: β = 94.5-97.0°, M4: β = 88.0-92.0° phases with α-$Mg_2V_2O_7$ structure) is slightly different at 600 and 800°C in the conditions of this study. This slight difference between the two crystalline phases with the same structure is evidenced with differences in unit cell parameters values obtained. In $Mg_yCu_{2-y}V_2O_7$ compositions fired at 600°C,

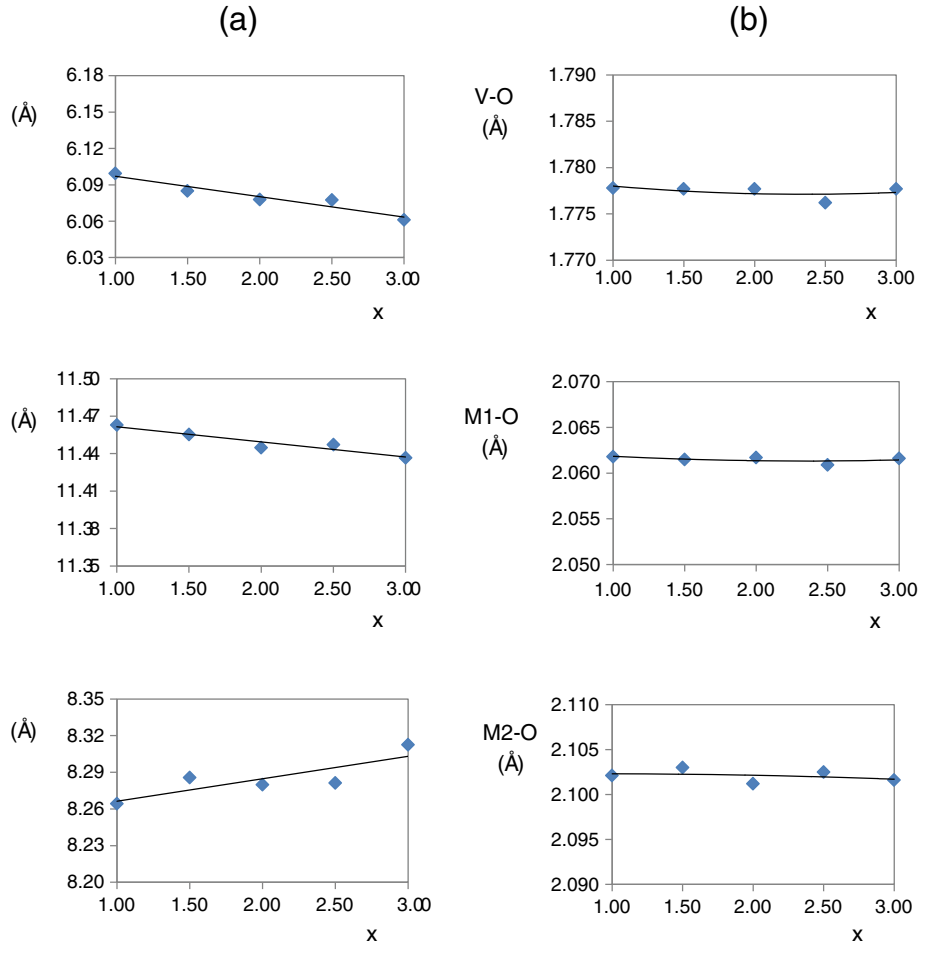

Figure 4 Cell parameters in the $Mg_3V_2O_8$ structure. Variation of unit cell parameters **(a)** and interatomic distances **(b)** in Mg orthovanadate structure with composition obtained from $Mg_xCu_{3-x}V_2O_8$ samples fired at 1000°C/1 h.

the values of a and β parameters decrease when y increases in β-$Cu_2V_2O_7$ structure (crystalline phase is obtained with a weight fraction > 35% when $0.25 \leq y \leq 1.5$). At 800°C this crystalline phase is obtained with a weight fraction > 35% only when $0.5 \leq y \leq 0.75$. In crystalline phase with α-$Mg_2V_2O_7$ structure, β angle value is close to 100° at 300°C and it is close to 90° at 800°C. When two crystalline phases with this structure are detected in the same sample, unit cell parameters are 0.2 Å (a, b, c parameters) or 8 degrees (β parameter) longer and wider in one of them. This fact is in accordance with the formation of solid solutions in this monoclinic α-$Mg_2V_2O_7$ structure with the replacement of Mg (II) ion by Cu (II) and with an important distortion structural in these formed solid solutions. Solid solutions with monoclinic α-$Mg_2V_2O_7$ structure are obtained when $0.5 \leq y \leq 2.0$ at 600 and 800°C. At 1000°C, these last solid solutions are obtained when $y \geq 1.5$, including all unmelted samples (Table 9).

Coordination number of V (V) ion in Cu and Mg orthovanadate and divanadate structures is four. Coordination number of Cu (II) ion is four and five and coordination number of Mg (II) ion is six in these structures. Values obtained from samples are in accordance with literature about these structures. In distorted monoclinic structure of $Cu_3V_2O_8$ obtained from $Mg_2CuV_2O_8$ composition at 800°C, the coordination number of Cu (II) and Mg (II) ions are also six.

Average interatomic V-O distances is smaller than average interatomic Cu-O or Mg-O distances in all of detected crystalline phases. Figure 5 shows the average interatomic V-O and Cu-O or Mg-O distances obtained from $Mg_yCu_{2-y}V_2O_7$ compositions considering all the crystalline phases in each composition and its weight fraction in samples fired at 600, 800 and 1000°C. These M-O (M = Cu, Mg) interatomic distances increase with magnesium amount (y) when $0 \leq y \leq 1.25$. This increased average M-O distance is coincident with destabilization of structures of Cu divanadate and a change is observed when $y > 1.25$. Structures of Cu divanadate are unstable with temperature and structures of Mg divanadates are stable at 1000°C when $1.5 \leq y \leq 2.0$ (Table 3).

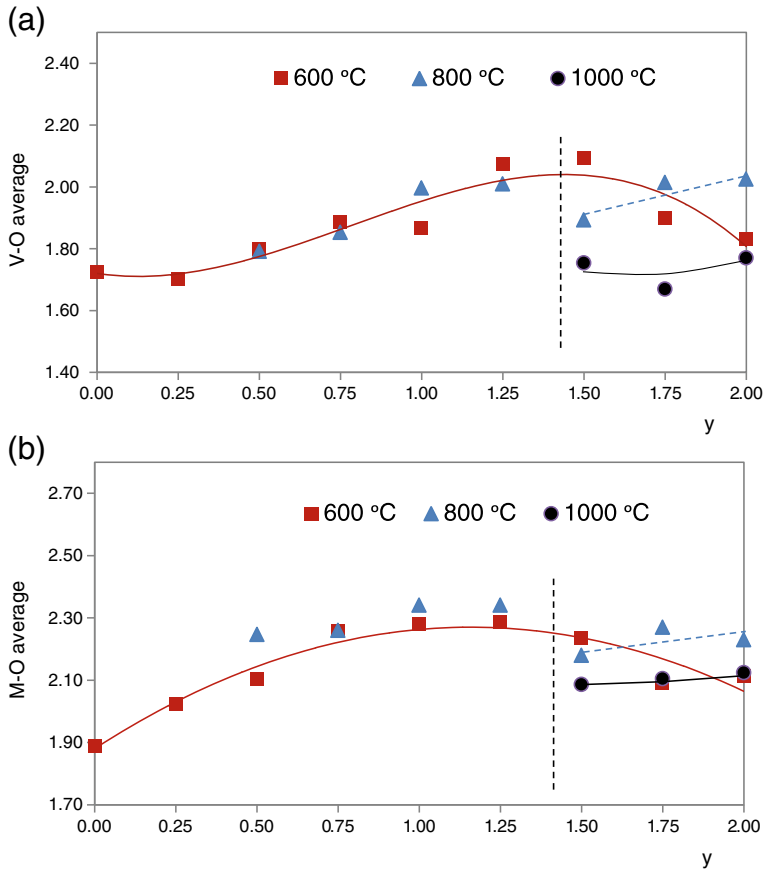

Figure 5 Interatomic distances in $Mg_yCu_{2-y}V_2O_7$ compositions. Average interatomic V-O **(a)** and M-O **(b)** distances in $Mg_yCu_{2-y}V_2O_7$ ($0 \leq y \leq 1$) compositions fired at 600°C/12 h, 800°C/1 h and 1000°C/1 h considering weight fraction of crystalline phases.

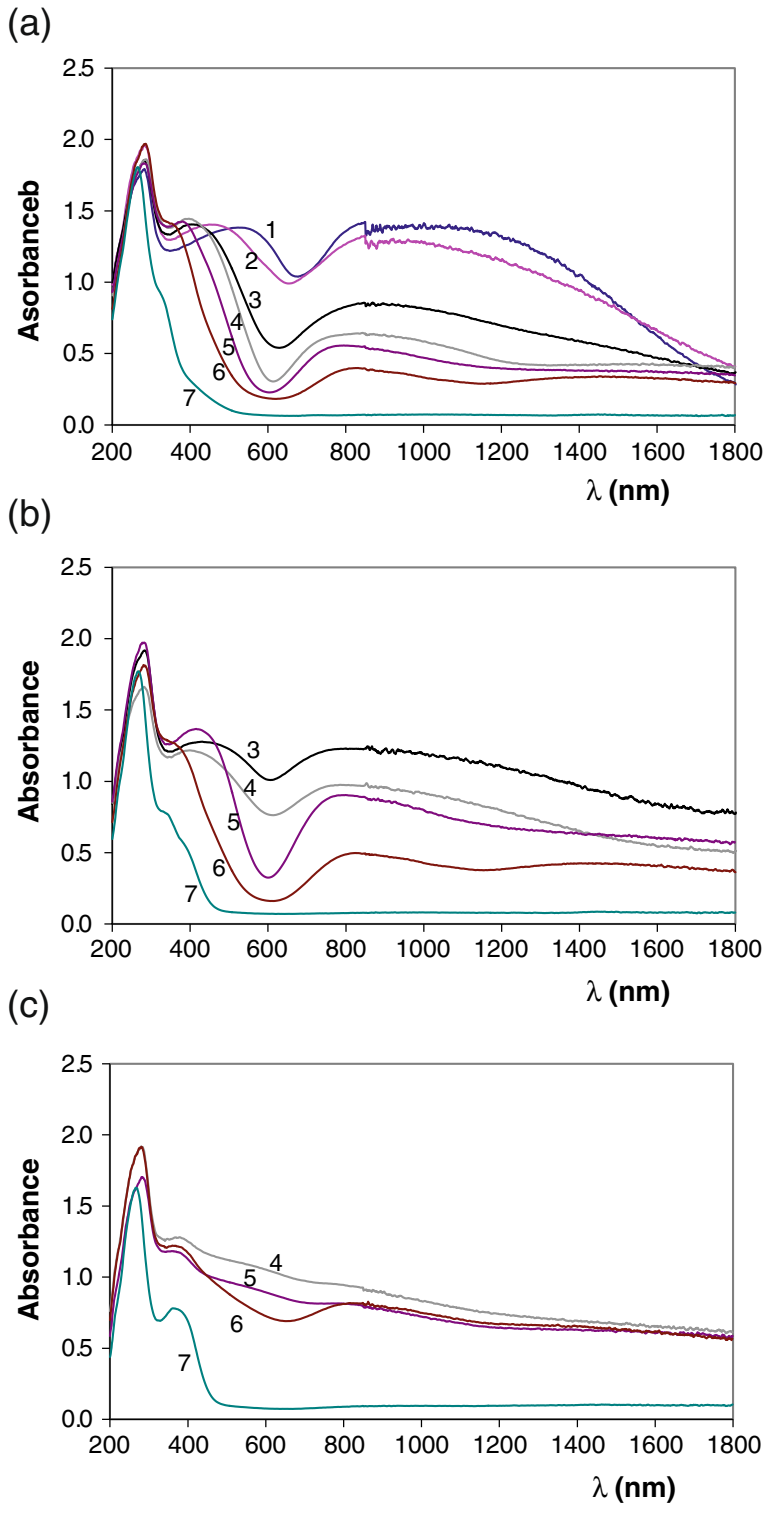

Figure 6 Variation of UV–vis-NIR spectra from $Mg_xCu_{3-x}V_2O_8$ compositions. UV–vis-NIR spectra of $Mg_xCu_{3-x}V_2O_8$ ($0.0 \leq x \leq 3.0$) samples fired at: **(a)** 600, **(b)** 800 and **(c)** 1000 °C; x = 0.0 (1), x = 0.5 (2), x = 1.0 (3), x = 1.5 (4), x = 2.0 (5), x = 2.5 (6) and x = 3.0 (7).

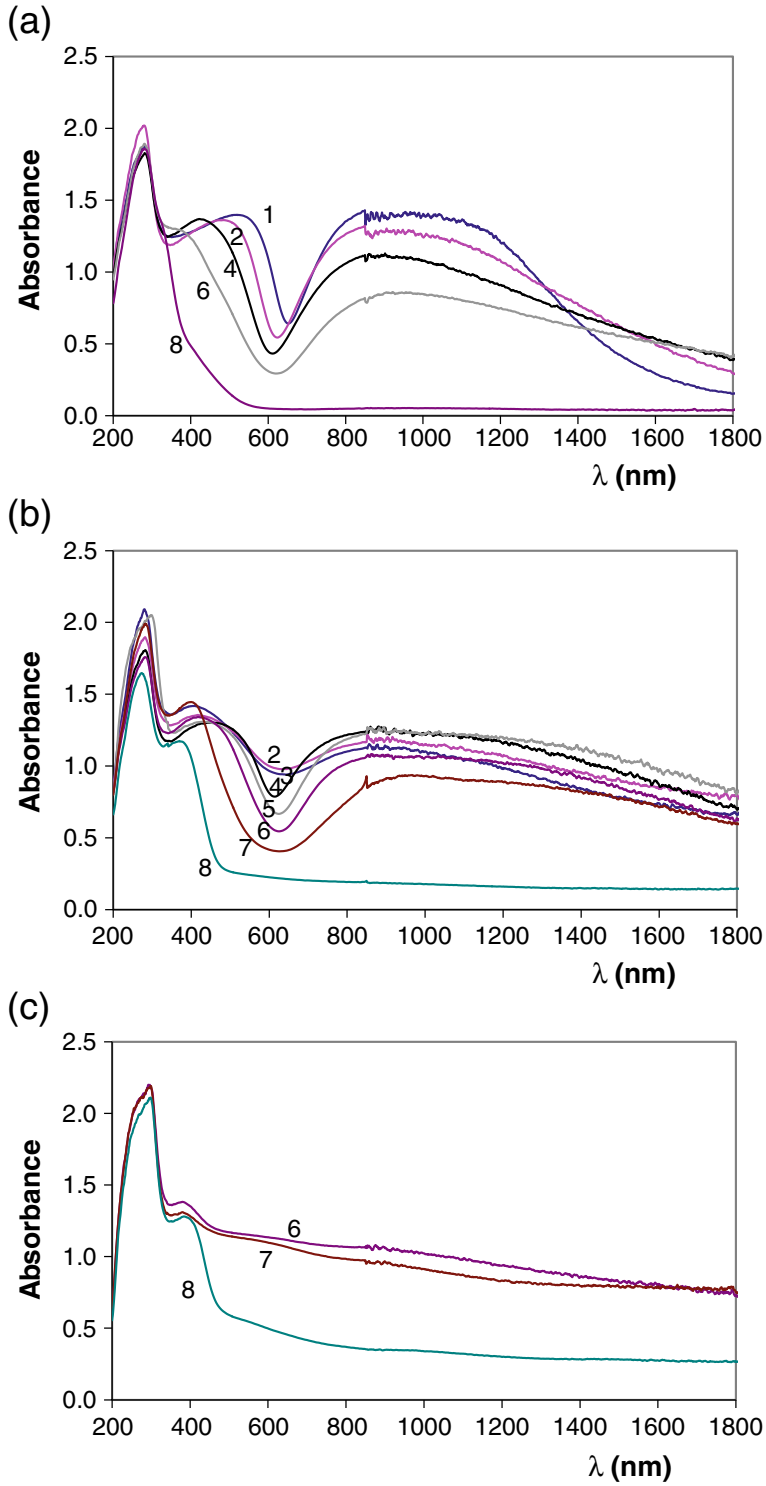

Figure 7 Variation of UV–vis-NIR spectra from $Mg_yCu_{2-y}V_2O_7$ compositions. UV–vis-NIR spectra of $Mg_yCu_{2-y}V_2O_7$ ($0.0 \leq y \leq 2.0$) samples fired at : **(a)** 600, **(b)** 800 and **(c)** 1000 ºC; y = 0.0 (1), y = 0.50 (2), y = 0.75 (3), y = 1.0 (4), y = 1.25 (5), y = 1.50 (6), y = 1.75 (7) and y = 2.0 (8).

Figures 6 and 7 show UV–vis-NIR spectra of $Mg_xCu_{3-x}V_2O_8$ ($0 \le x \le 3$) and $Mg_yCu_{2-y}V_2O_7$ ($0 \le y \le 2$) compositions fired at 600, 800 and 1000°C. Visible spectra obtained from $Mg_yCu_{2-y}V_2O_7$ ($0 \le y \le 2$) compositions fired at 800°C/1 h and $Mg_xCu_{2-x}P_2O_7$ ($0 \le x \le 1.5$) compositions fired at 800°C/5d (Tena 2012) are shown in Figure 8. Most of complex with Cu (II) ion are formed with four ligands (IC = 4). The reason for the unusual behaviour is connected with the Jahn-Teller effect. Because of that, the Cu (II) ions do not bind the fifth and sixth ligands strongly. Structural distortion due to this Jahn-Teller effect can explain the asymmetry in observed bands. From Cu (II) ion (d^9) a transition d-d is allowed. Experimentally electronic spectra of Cu (II) ion are often characterized by a single highly asymmetric band. In this study spectra show a strong absorbance in 700–1400 nm wavelength range with the absorption maximum at 800–900 nm. It can be associated with Cu (II) d-d transition. Bands due to d-d transitions are not expected from V (V) ion. Strong absorbance in 430–600 nm wavelength range (in visible wavelength range) with the absorption maximum depending of copper amount in the sample (x or y values) is detected in $Mg_xCu_{3-x}V_2O_8$ ($0 \le x \le 3$) and $Mg_yCu_{2-y}V_2O_7$ ($0 \le y \le 2$)

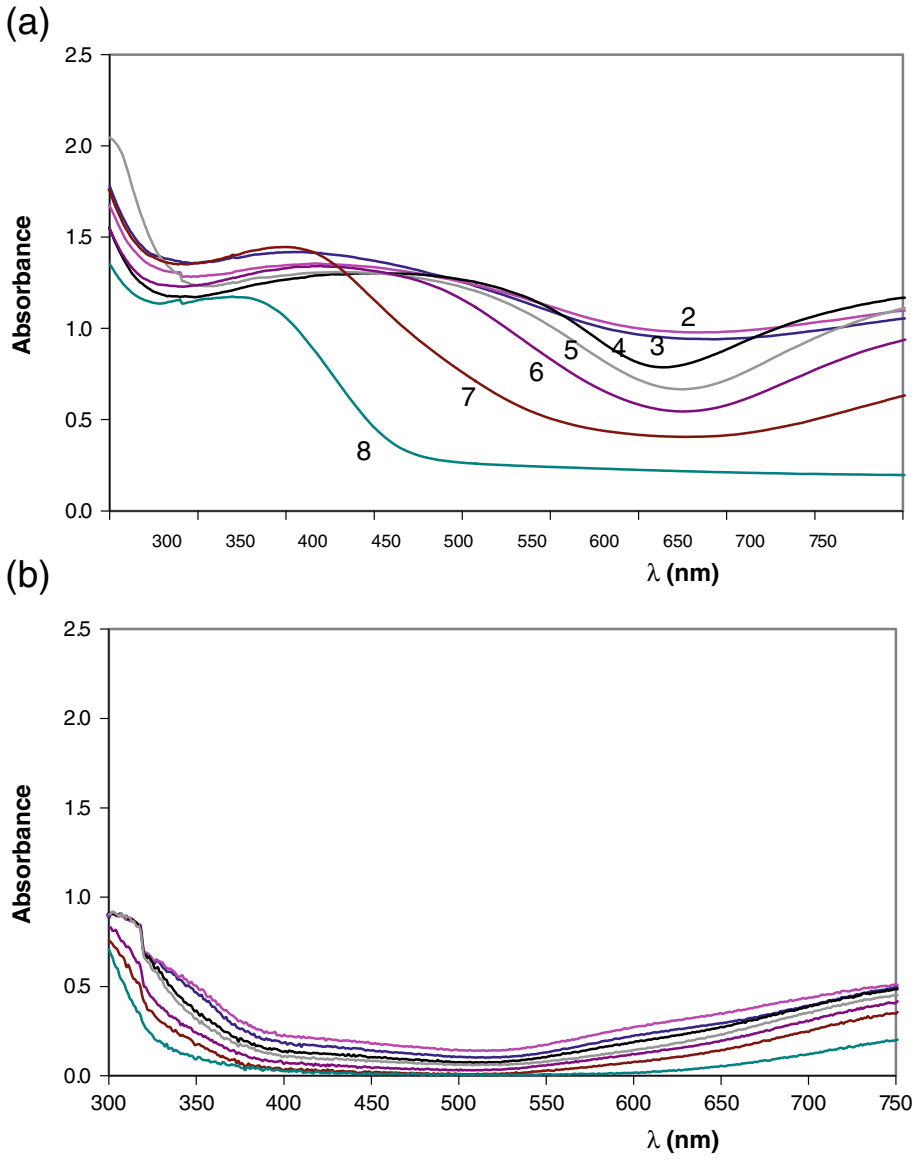

Figure 8 Visible spectra of compositions at 800°C. Visible spectra of: **(a)** $Mg_yCu_{2-y}V_2O_7$ ($0.0 \le y \le 2.0$) and **(b)** $Mg_xCu_{2-x}P_2O_7$ ($0.0 \le x \le 1.5$) samples fired at 800°C; y = 0.50 (2), y = 0.75 (3), y = 1.00 (4), y = 1.25 (5), y = 1.50 (6), y = 1.75 (7), y =2.00 (8).

compositions at 300°C/12 h, 600°C/12 h, 800°C/1 h and 1000°C/1 h. The strong absorbance in 350–600 nm wavelength range is not observed in $Mg_xCu_{2-x}P_2O_7$ compositions (Figure 8) and in $Mg_xCu_{3-x}V_2O_8$ (x = 3) and $Mg_yCu_{2-y}V_2O_7$ (y = 2) compositions. It is associated with charge transfer between Cu-O in orthovanadates and divanadates when $0 \le x < 3$ or when $0 \le y < 2$. When x = 3 or y = 2, the charge transfer is associated with V-O charge transfer ($\lambda < 430$ nm in studied temperature range). Maximum of this band is observed at higher wavelength when copper amount is hight than when the copper amount is low. This strong absorbance in visible wavelength range explains the colour of these materials. At 600 and 800°C, coloration from samples with vanadate structures is red-brown, orange and yellow and is very different to the weak blue coloration obtained from samples with phosphate structures (Tena 2012). At 1000°C, brown-dark and black colorations are obtained when $x < 3.0$ or $y < 2.0$ and a strong absorbance in 400–1800 nm range is obtained in spectra. In the most of samples band due to d-d transition and band due to charge transfer can not be differentiated at 1000°C. Vanadate structure does not seem to be the only important factor for the presence of this charge transfer band because it is present in $Mg_xCu_{3-x}V_2O_8$ ($x \neq 3$) compositions and in $Mg_xCu_{2-y}V_2O_7$ ($y \neq 2$) compositions with different crystalline phases detected by XRD (Tables 2 and 3). The difference of coloration of Cu phosphates and Cu vanadates might be explained from differences in interatomic Cu-O distances due to the presence of bonds P-O or V-O. Interatomic Cu-O distances are smaller in vanadate structures than in phosphate structures (Cu-O bond is more strong in vanadates than in phosphates) because the V-O bond is weaker than the P-O bond (interatomic V-O distances are slightly greater than interatomic P-O distances). Table 10 shows interatomic distances in some of these compositions.

CIE L*, a* and b* parameters of $Mg_xCu_{3-x}V_2O_8$ ($0 \le x \le 3$) and $Mg_yCu_{2-y}V_2O_7$ ($0 \le y \le 2$) samples fired at 600, 800 and 1000°C are shown in Table 11.

Interesting yellow colorations are obtained when x = 1.5 and 2.0 at 600°C/12 and when x = 2.0 at 800°C/1 h. In these samples that development yellow colorations, crystalline phase with monoclinic $Cu_3V_2O_8$ structure is detected. The best yellow colour is obtained from $Mg_2CuV_2O_8$ (x = 2.0) solid solution with monoclinic $Cu_3V_2O_8$ structure. This is the only crystalline phase detected at 800°C in conditions of this study. The Mg (II) incorporated into this structure stabilizes this crystalline phase at temperatures higher than 780°C (melting point of $Cu_3V_2O_8$). In $Mg_2CuV_2O_8$ composition fired at 800°C, average distances of M1-O (M1 = Cu, Mg) = 1.9587 Å and M2-O (M2 = Cu, Mg) = 2.1129 Å are obtained. Yellow colorations are not obtained from Cu, Mg divanadates.

Table 10 Interatomic distances in orthovanadates, divanadates and diphosphates of Cu and Mg

Composition	Mg^{2+}-O (Å)	Cu^{2+}-O (Å)	V-O or P-O (Å)
[1] $Cu_3V_2O_8$	———	1.912 (4) - 1.988 (5)	1.643 (3) - 1.795 (4)
[1] $Cu_3P_2O_8$	———	1.925 (3) - 1.981 (3)	1.510 (2) - 1.572 (2)
[1] $Mg_3V_2O_8$	2.022 (1) - 2.135 (1)	———	1.695 (1) - 1.809 (1)
[1] $Mg_3P_2O_8$	1.965 (8) - 2.142 (7)	———	1.527 (5) - 1.535 (8)
[2] $Mg_xCu_{3-x}V_2O_8$	1.880 (2) - 2.306 (1)		1.570 (3) -1.972 (2)
[1] $Cu_2V_2O_7$	———	1.880 (5) - 2.542 (4)	1.644 (7) - 1.770 (4)
[1] $Cu_2P_2O_7$	———	1.929 (1) - 2.313 (1)	1.437 (1) - 1.561 (1)
[1] $Mg_2V_2O_7$	1.992 (3) - 2.221 (3)	———	1.629 (3) - 1.817 (4)
[1] $Mg_2P_2O_7$	1.850 (1) - 2.381 (1)	———	1.543 (1) - 1.785 (1)
[2] $Mg_yCu_{2-y}V_2O_7$	1.862 (3) - 2.282 (1)		1.620 (2) - 1.904 (4)
[3] $Mg_xCu_{2-x}P_2O_7$	1.927 (3) - 2.282 (2)		1.495 (2) - 1.574 (1)

[1] Inorganic Crystal Structure Database (ICSD) (2013).
[2] $Mg_xCu_{3-x}V_2O_8$ ($0 \le x \le 3$) and $Mg_yCu_{2-y}V_2O_7$ ($0 \le y \le 2$) compositions prepared in this study.
[3] (Tena 2012).

The colour red-brown obtained from $Mg_{0.5}Cu_{1.5}V_2O_7$ (y = 0.5) fired at 600°C /12 h is the most noticeable colour but it is unstable at 800°C /1 h. Dark brown colour is obtained from this composition at 800°C. The major crystalline phase detected by XRD is the crystalline phase with β-$Cu_2V_2O_7$ structure in this sample fired at 600°C.

Orange colour is obtained when y = 0.75, 1.00 and 1.25 at 600°C/12 h and when y = 1.25 and 1.50 at 800°C/1 h. In these orange materials, a mixture of monoclinic crystalline phases with β-$Cu_2V_2O_7$ and $Cu_3V_2O_8$ or β-$Cu_2V_2O_7$ and α-$Mg_2V_2O_7$ structures is detected by XRD.

Figure 9 shows the wavelength of charge transfer in $Mg_yCu_{2-y}V_2O_7$ compositions fired at 600°C/12 h (bands in Figure 7 (a)) and the variation of average V-O and M-O distances with wavelength of charge transfer and with composition (y). Inflection point between maximum and minimum absorbance in band is considered in assignation of wavelength values. Distances are calculated considering all the crystalline phases detected by XRD in each composition and its weight fraction in this sample. When Cu (II) amount (y) decreases in samples, the wavelength of charge transfer decreases in all compositions at this temperature and colour of samples changes from red-brown to yellow. From variation of average interatomic distances at 600°C/12 h, the longest average M-O distances is detected when $0.75 \le y \le 1.25$ and orange coloration is obtained in these materials (charge transfer about 550 nm). At this temperature red-brown coloration is obtained in samples with the shortest average M-O distances (charge transfer about 570 nm). The obtained colorations are different with similar average

Table 11 CIE L* a* b* colour parameters in $Mg_xCu_{3-x}V_2O_8$ ($0 \le x \le 3$) and $Mg_yCu_{2-y}V_2O_7$ ($0 \le y \le 2$) samples

x	Observed colour	$Mg_xCu_{3-x}V_2O_8$ samples fired at 600°C/12 h		
		L*	a*	b*
0.00	dark brown	41.57	4.10	0.79
0.50	dark brown	43.59	5.83	6.82
1.00	orange	56.94	13.29	25.79
1.50	yellow	66.67	18.29	42.22
2.00	yellow	76.77	6.47	47.76
2.50	light brown	83.12	- 1.34	35.49
3.00	light yellow	94.76	- 2.00	13.35
y	**Observed colour**	**$Mg_yCu_{2-y}V_2O_7$ samples fired at 600°C/12 h**		
		L*	**a***	**b***
0.00	dark brown	43.33	13.86	4.91
0.25	red-brown	38.34	20.54	9.80
0.50	red-brown	50.60	21.72	16.23
0.75	orange	46.88	25.71	29.13
1.00	orange	58.96	19.05	30.90
1.25	orange	57.06	19.77	46.16
1.50	brown	70.76	10.83	36.19
1.75	light brown	69.70	4.76	34.91
2.00	light yellow	92.46	- 1.35	22.95
x	**Observed colour**	**$Mg_xCu_{3-x}V_2O_8$ samples fired at 800°C/1 h**		
		L*	**a***	**b***
1.00	dark brown	46.73	3.03	6.73
1.50	brown	53.37	4.77	15.20
2.00	yellow	68.97	12.02	41.84
2.50	light yellow	83.96	0.38	39.86
3.00	light yellow	95.50	- 3.57	11.54
y	**Observed colour**	**$Mg_yCu_{2-y}V_2O_7$ samples fired at 800°C/1 h**		
		L*	**a***	**b***
0.50	dark brown	48.90	4.19	10.50
0.75	dark brown	47.58	3.95	8.75
1.00	brown	49.18	10.31	11.09
1.25	orange	52.11	13.11	16.37
1.50	orange	57.13	13.67	24.55
1.75	light brown	69.05	3.87	35.70
2.00	light brown	85.00	- 5.37	22.14
x	**Observed colour**	**$Mg_xCu_{3-x}V_2O_8$ samples fired at 1000°C/1 h**		
		L*	**a***	**b***
1.00	grey	52.75	0.96	0.56
1.50	dark brown	48.74	1.15	4.58
2.00	dark brown	51.37	1.46	6.09
2.50	brown	58.02	2.69	12.51
3.00	yellow	94.28	- 4.86	17.95

Table 11 CIE L* a* b* colour parameters in $Mg_xCu_{3-x}V_2O_8$ ($0 \le x \le 3$) and $Mg_yCu_{2-y}V_2O_7$ ($0 \le y \le 2$) samples *(Continued)*

y	Observed colour	$Mg_yCu_{2-y}V_2O_7$ samples fired at 1000°C/1 h		
		L*	a*	b*
1.50	black	46.85	- 0.16	3.84
1.75	black-brown	47.39	0.31	3.86
2.00	yellow-brown	67.25	- 1.12	20.11

distances when Mg amount is high ($y > 1.25$) and when Cu amount is high ($y < 1.25$) because Mg (II) and Cu (II) radius are similar. Structural changes must be also considered to explain the complete evolution of colour with composition.

Conclusions

From $Mg_xCu_{3-x}V_2O_8$ compositions solid solutions with triclinic $Cu_3V_2O_8$ structure are obtained in $0.0 \le x \le 1.0$ at 600°C. When $x = 1.0$, $MgCu_2V_2O_8$ compound is detected at 800°C. When $x = 2.0$, $Mg_2CuV_2O_8$ compound with the ordered metal distributions is not detected in the conditions of this study. From this composition, solid solutions with monoclinic $Cu_3V_2O_8$ structure (Cu1 in 2b sites) are obtained. These solid solutions with monoclinic $Cu_3V_2O_8$ structure are obtained when $1.5 \le x \le 2.0$ at 600°C and 800°C. Solid solutions with orthorhombic $Mg_3V_2O_8$ structure are obtained when $2.5 \le x \le 3.0$ at 600, 800°C and when $1.0 \le x \le 3.0$ at 1000°C. In this study, the most stable solid solutions are obtained with Mg orthovanadate structure (orthorhombic).

From $Mg_yCu_{2-y}V_2O_7$ compositions, the formation of two kind of solid solutions with β-$Cu_2V_2O_7$ and α-$Mg_2V_2O_7$ structures is detected. Solid solutions with monoclinic β-$Cu_2V_2O_7$ structure are obtained when $0.25 \le y \le 1.50$ at 600°C and when $0.50 \le y \le 0.75$ at 800°C. Solid solutions with monoclinic α-$Mg_2V_2O_7$ structure are obtained when $0.5 \le y \le 2.0$ at 600 and 800°C and showing an important structural distortion. At 1000°C, solid solutions with α-$Mg_2V_2O_7$ structure are obtained in $1.5 \le y \le 2.0$ compositional range. It is proposed the existence of a new polymorph of $Mg_2V_2O_7$ compound with α-$Mn_2V_2O_7$ structure detected when $y \ge 1.25$ at 300°C.

Strong absorbance in visible spectra is detected in $Mg_xCu_{3-x}V_2O_8$ ($0 \le x < 3$) and $Mg_yCu_{2-y}V_2O_7$ ($0 \le y < 2$) compositions which is associated with charge transfer between Cu-O in orthovanadates and divanadates. Wavelength of the abrupt change in absorbance is in accordance with Cu-O interatomic distances in these

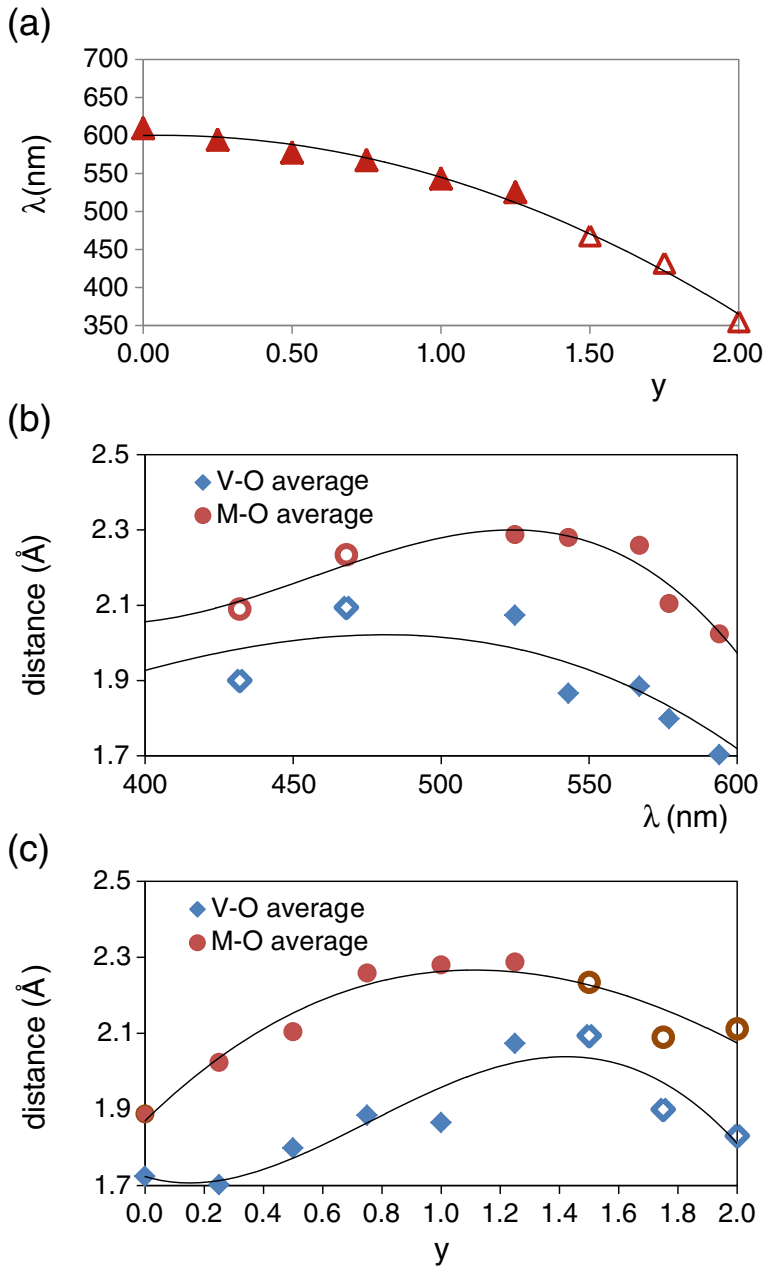

Figure 9 Variation of interatomic distances with wavelength and composition. Variation of wavelength of Cu-O charge transfer with composition **(a)**, variation of average interatomic V-O and M-O (M = Cu, Mg) distances with wavelength **(b)** and variation of these average interatomic distances with composition **(c)** from $Mg_yCu_{2-y}V_2O_7$ samples fired at 600°C. Solid marks: y < 1.5; Empty marks: y ≥ 1.5.

structures. In this study, the best yellow colour is obtained from $Mg_2CuV_2O_8$ (x = 2.0) solid solution with monoclinic $Cu_3V_2O_8$ structure. The colour red-brown is obtained from $Mg_{0.5}Cu_{1.5}V_2O_7$ (y = 0.5) fired at 600°C /12 h and it is unstable at 800°C /1 h. This red-brown colour is obtained when the average M-O distances are the shortest from divanadates. Orange colour is also obtained from some divanadates when average M-O distance is long.

Structural changes must be also considered to explain the colour of these materials. Thus, yellow colorations are obtained from orthovanadates and red-brown and orange colorations are obtained from divanadates.

Additional files

Additional file 1: Information about crystal structures.

Additional file 2: XRD patterns from $Mg_xCu_{3-x}V_2O_8$ compositions.
Additional file 3: XRD patterns from $Mg_yCu_{2-y}V_2O_7$ compositions.

Competing interests
The authors declare that they have no competing interests.

Authors' contributions
Both authors read and approved the final manuscript.

Acknowledgements
The authors acknowledge the financial support given by the government of Spain, MAT 2008–02893, MAT 2010–15094 and MAT2013-40950-R projects.

Author details
[1]Inorganic Chemistry Area, Inorganic and Organic Chemistry Department, Jaume I University, P.O. Box 224, Castellón, Spain. [2]Physical Chemistry Area, Physical and Analytical Chemistry Department, Oviedo University-CINN, Oviedo, Spain.

Received: 22 November 2014 Accepted: 26 February 2015
Published online: 03 April 2015

References

Boultif A, Loüer D (2007). Dicvol computer program, version 06.
Calvo C, Faggiani R (1975) α cupric divanadate. Acta Cryst B31:603–605
Chapon L, Rodriguez-Carvajal J (2008). FPStudio computer program, version 2.0.
Clark GM, Morley R (1976) System MgO-V_2O_5. J Solid State Chem 16(3–4):429–435
Coing-Boyat J (1982) Structure de la variété ordinaire, triclinique, de l'orthovanadate de cuivre (II), Cu_3 $(VO_4)_2$. Acta C ryst B38:1546–1548
Commission Internationale del'Eclairage (CIE) (1971) Recommendations on uniform color spaces, color difference equations, Phychometrics color terms. Suplement n° 2 of CIE Publication N° 15 (E1-1.31), Bureau Central de la CIE, Paris
Fleury P (1966) System V_2O_5-CuO in O_2. C.R. Acad Sci Ser C 263(22):1375
García A, Llusar M, Calbo J, Tena MA, Monrós G (2001) Low-toxicity red ceramic pigments for porcelainised stoneware from lanthanide-cerianite solid solutions. Green Chem 3:238–242
Gopal R, Calvo C (1974) Crystal structure of magnesium divanadate, $Mg_2V_2O_7$. Acta Cryst B30:2491–2493
Inorganic Crystal Structure Database (ICSD) (2013) Fachinformationszentrum. FIZ, Karlsruhe, Germany
Krishnamachari N, Calvo C (1971) Refinement of the structure of Mg_3 $(VO_4)_3$. Can J Chem 49:1629–1637
Mercurio-Lavaud D, Bernard Frit M (1973) Structure crystalline de la variété haute temperature du pyrovanadate de cuivre: $Cu_2V_2O_7$ β. C R Acad Sc Paris, t 277(Série C):1101–1104
Rietveld HM (1969) A profile refinement method for nuclear and magnetic structures. J Appl Cryst 2:65–71
Rodriguez-Carvajal J (2012). Fullprof.2 k computer program, version 5.00, France.
Shannon RD, Calvo C (1972) Crystal structure of a New form of $Cu_3V_2O_8$. Can J Chem 50:3944–3949
Sorlí S, Tena MA, Badenes JA, Llusar M, Monrós G (2004) Study of nickel precursors in (Ni, M, Ti) O2 (M = Sb, Nb) yellow ceramic pigments. Br Ceram Trans 103:10–14
Tena MA (2012) Characterization of $Mg_xM_{2-x}P_2O_7$ (M = Cu and Ni) solid solutions. J Eur Ceram Soc 32(2):389–397, doi: 10.1016/j.jeurceramsoc.2011.09.018
Tena MA, Mestre A, García A, Sorlí S, Monrós G (2003) Synthesis of gray ceramic pigments with rutile structure from alkoxides. J Sol–gel Sci and Techn 26:813–816
West AR (1984) Solid state chemistry and its applications. John Wiley & Sons, Chichester